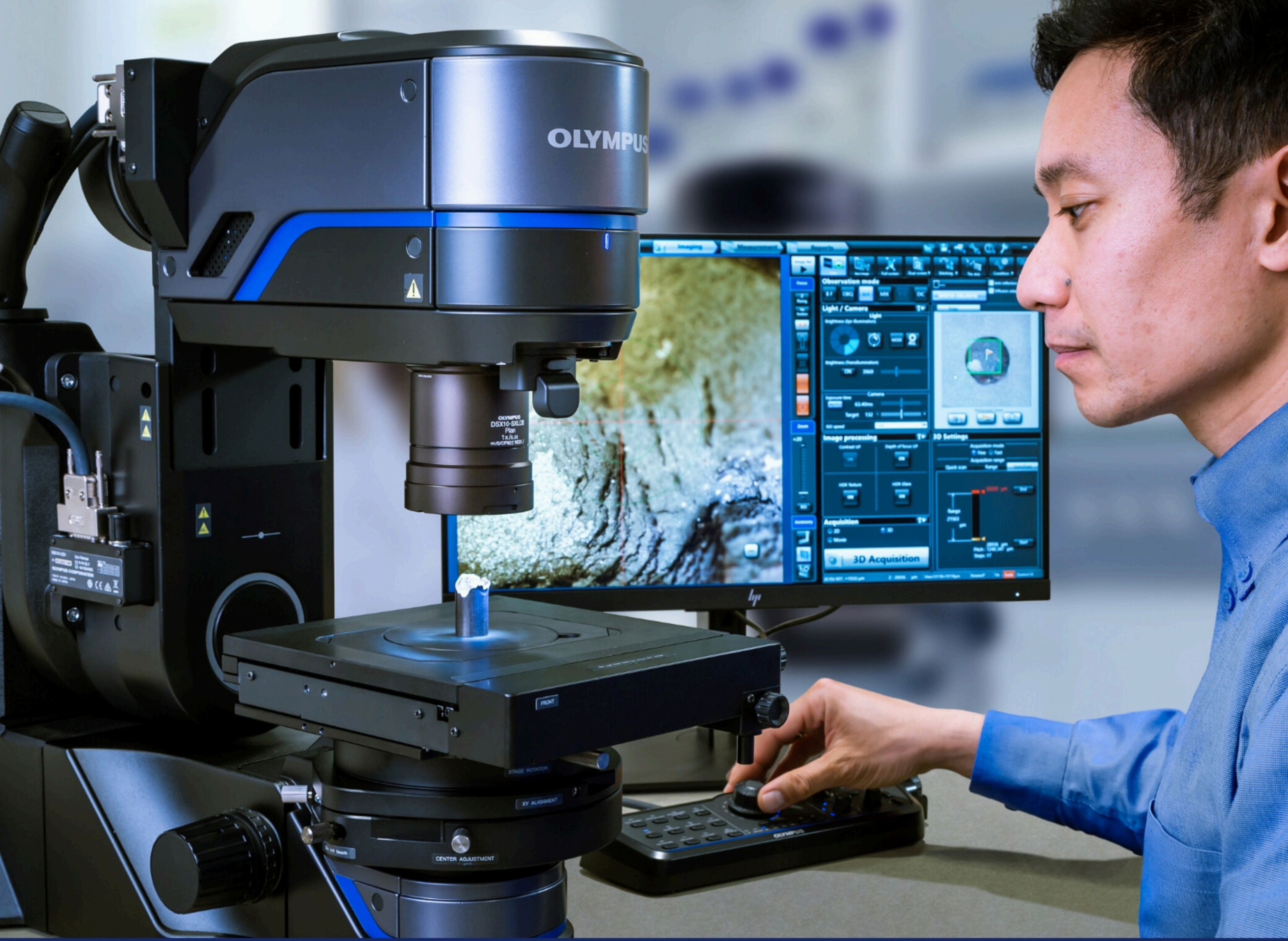

Science Meets Technology with Advanced Optical Metrology

Access in-depth information on methods and applications in the R&D field of optical metrology through free to access article digests of recent peer-reviewed publications and more.

Discover advancedopticalmetrology.com now!

OLYMPUS

WILEY

ADVANCED ENERGY MATERIALS
www.advenergymat.de

Check for updates

Hybrid All-in-One Power Source Based on High-Performance Spherical Triboelectric Nanogenerators for Harvesting Environmental Energy

Lingyi Xu, Liang Xu, Jianjun Luo, Ying Yan, Bei-Er Jia, Xiaodan Yang, Yihua Gao, and Zhong Lin Wang**

With the development of the Internet of Things (IoTs), widely distributed electronics in the environment require effective in situ energy harvesting technologies, which is made challenging by the unstable supply and severe conditions in some environments. In this work, a hybrid all-in-one power source (AoPS) is demonstrated for widely adaptive environmental energy harvesting. With a novel structure, the AoPS hybridizes high-performance spherical triboelectric nanogenerators (TENGs) with solar cells, enabling the harvesting of most typical environmental energies from wind, rain drops, and sun light, for complementary supply. The spherical TENG units with a packaged structure can work robustly to collect energy from fluid. Nearly continuous direct current and a high average power of 5.63 mW can be obtained by four TENG units, which is further complemented by solar cells. Typical application scenarios are also demonstrated, achieving self-powered soil moisture control, forest fire prevention and pipeline monitoring. The work realizes the concept of an environmental power source that can be deployed in the environment with high adaptability to make use of all kinds of surrounding energies for powering electronics in all-weather conditions, providing a reliable foundation for the era of the IoTs.

1. Introduction

With the rapid development of Internet of Things (IoTs), widely distributed electronics in the environment can launch various application fields ranging from intelligent farm, infrastructure monitoring to environmental protection.[1–3] However, the power supply of such electronic devices arises as a fundamental problem, due to their possible distribution in inaccessible areas or even closed environments such as forests or pipelines. At present, traditional power supply such as battery is mainly adopted, which needs replacement or recharging and can cause great difficulty in maintenance. Meanwhile, a battery itself can be a source of environmental pollution.[4] Therefore, it is highly desired to develop a maintenance-free, reliable power source that can be widely adaptive to different environments.

Invented in 2012, triboelectric nanogenerators (TENGs, also called Wang generator) have been demonstrated as an effective approach to convert ambient mechanical energy into electricity.[5–11] Based on the tribo-electrification effect and the electrostatic induction, the TENG owes merits of simple structure, easy fabrication, diverse material options, and low cost.[12,13] Through proper structure design, the TENG can be applied to a wide range of situations and harvest various low-frequency mechanical energies, such as human motion, vibration, wind, rain and water wave.[8,14–21] Thus, the TENG technology can provide a possible solution for maintenance-free power supply in IoTs, which can further combine with energy storage devices, such as capacitors, to

L. Y. Xu, Prof. Y. Gao
Center for Nanoscale Characterization and Devices (CNCD)
Wuhan National Laboratory for Optoelectronics (WNLO) and School of Physics
Huazhong University of Science and Technology (HUST)
Wuhan 430074, China
E-mail: gaoyihua@hust.edu.cn

Prof. L. Xu, Dr. J. Luo, X. Yang, Prof. Z. L. Wang
CAS Center for Excellence in Nanoscience
Beijing Key Laboratory of Micro-Nano Energy and Sensor
Beijing Institute of Nanoenergy and Nanosystems
Chinese Academy of Sciences
Beijing 100083, China
E-mail: zhong.wang@mse.gatech.edu

The ORCID identification number(s) for the author(s) of this article can be found under https://doi.org/10.1002/aenm.202001669.

DOI: 10.1002/aenm.202001669

Prof. L. Xu, Dr. J. Luo, X. Yang, Prof. Z. L. Wang
School of Nanoscience and Technology
University of Chinese Academy of Sciences
Beijing 100049, China

Prof. Y. Yan
Key Laboratory for Precision and Nontraditional Machining Technology of Ministry of Education
Dalian University of Technology
Dalian 116024, China

B.-E. Jia
School of Materials Science and Engineering
Zhejiang University
Hangzhou 310027, China

Prof. Z. L. Wang
School of Materials Science and Engineering
Georgia Institute of Technology
Atlanta, GA 30332, USA

© 2020 Wiley-VCH GmbH

achieve self-powered systems.[22–27] However, although there are lots of attempts in this field, the proposed devices are usually dependent on single energy source, which cannot ensure reliable power supply. Some recently reported hybrid devices have also been attempted to harvest multiple forms of environmental energy, but they are not suitable for working in all-weather harsh environment, and their output power still needs to be further improved for practical applications.[28–32] The most typical environmental energy sources, such as wind, rain drop and sun light, are usually unstable with time and unevenly distributed in different sites.[33] Some environments have high humidity that is generally detrimental to the performance of TENGs.[34] Therefore, for practical applications, devices that can effectively harness all major environmental energy forms simultaneously and work robustly in severe conditions is highly meaningful and significant, which can enable better merging of the electronics in the environment adopting in-situ energy harvesting for power.

Here, a hybrid all-in-one power source (AoPS) is demonstrated for widely adaptive environmental energy harvesting. With a novel structure, the AoPS hybridize high-performance spherical triboelectric nanogenerators with solar cells, enabling harvesting most typical environmental energies from wind, rain drop, and sun light simultaneously for complementary supply. The spherical TENG units with packaged structure can work robustly to collect fluid energy. The force and detailed fluid flow are also analyzed based on experiments and finite element method (FEM) calculation. Nearly continuous direct current and high average power of 5.63 mW can be obtained for four TENG units, and 1160 LEDs can be lighted up by the TENGs, which is further complemented by solar cells. Typical application scenarios are also demonstrated, achieving self-powered soil moisture control, forest fire prevention and pipeline monitoring. The work proposes and realizes the concept of environmental power source that can be well merged in the environment with high adaptability to supply electricity for electronics in all-weather condition, providing a reliable foundation for the era of IoTs.

2. Results and Discussion

2.1. Basic Concept of the All-in-One Power Source (AoPS) for Harvesting Environmental Energy

The concept of the AoPS is to develop a power source that can survive in different environment conditions and effectively harvest typical surrounding energies for electronics, sustaining self-powered systems that can conduct particular functions in the environment. A few features are essential for this device. First, although energy sources distribute widely in our environment, such as wind, sun light, and rain drop, they are usually unstable and cannot provide a continuous supply, imposing a "when" restriction. Meanwhile, the energy in some circumstances, such as in a tube, is limited to certain forms, imposing a "where" restriction. To overcome the "when" and "where" restrictions, the AoPS should have the capability to harvest energy from multiple sources simultaneously, because different sources have distinct distribution characteristics and can complement for each other. Moreover, the device must be robust and well packaged to be adaptive to various environments, especially those with a high humidity, which may affect the output of the device due to possible condensation of water on the surface.[35,36] **Figure 1**a depicts a general framework of the AoPS and the environmental self-powered system. All of the three common energy forms in the environment, from wind, rain, and sun, can be harnessed by the device. The harvested power goes through energy storage components to further suppress the fluctuation and then is supplied to sensors distributed in the environment. Consequently, a self-powered environmental monitoring system can be built. To make further extensions, a controller and different actuation terminals can also be integrated, achieving more complex functions in various application scenarios through recording and analyzing parameters of the environment, such as intelligent farm irrigation and forest fire prevention.

2.2. Structure and Working Principle of the AoPS

To realize the above features, the AoPS is designed based on hybridization of two types of energy harvesting components: TENG units and solar cells, as shown in Figure 1b. The TENG is used to harvest environmental mechanical energy, typically from fluid flow such as wind and rain. And the solar cell is for capturing the energy from light. In order to effectively and continuously collect fluid energy, a novel symmetrical structure of four arms is adopted, with one TENG unit on each arm of the acrylic frame. As shown in the enlarged view in Figure 1b, the TENG unit is basically a multilayer structure sealed in a spherical polypropylene (PP) shell, which is fabricated by stacking electrode disks and acrylic spacers (5 mm in thickness) one-by-one along a nylon rod. The copper layers on the disks and the spacers are interconnected to form two total electrodes on each hemisphere, which means that all electrode disks are connected in parallel. Fluorinated-ethylene-propylene (FEP) pellets are filled between the disks, occupying about half the space as a triboelectric material, and such amount of pellets is consistent with each electrode area and can maximize the output. A truncated-cone-shaped capture rim of polyethylene terephthalate (PET) is designed on each spherical TENG unit with fixed angle to catch and interact with the fluid. The spherical shape of the unit with the capture rim ensures that the force exerted by the fluid is much higher from the open direction of the rim. Due to that all the capture rims face the same direction (clockwise or counterclockwise), the net force from fluid on each capture rim will impose a torque toward the same direction via the arm, making the total structure to rotate around a flexible shaft of carbon fiber. Meanwhile, four commercial solar cells are fixed on two sides of the acrylic frame to collect solar energy.

The working mechanism of a single TENG unit is based on the conjugation of electrostatic induction and triboelectrification, and is in freestanding triboelectric-layer mode.[13] As shown in Figure 1c, when the TENG unit is rotated by external mechanical agitations, the orientation of the electrodes will change circularly, but the FEP pellets will always tend to stay near the bottom of the shell due to gravity. Thus they will have relative motion with the total electrodes, presenting

© 2020 Wiley-VCH GmbH

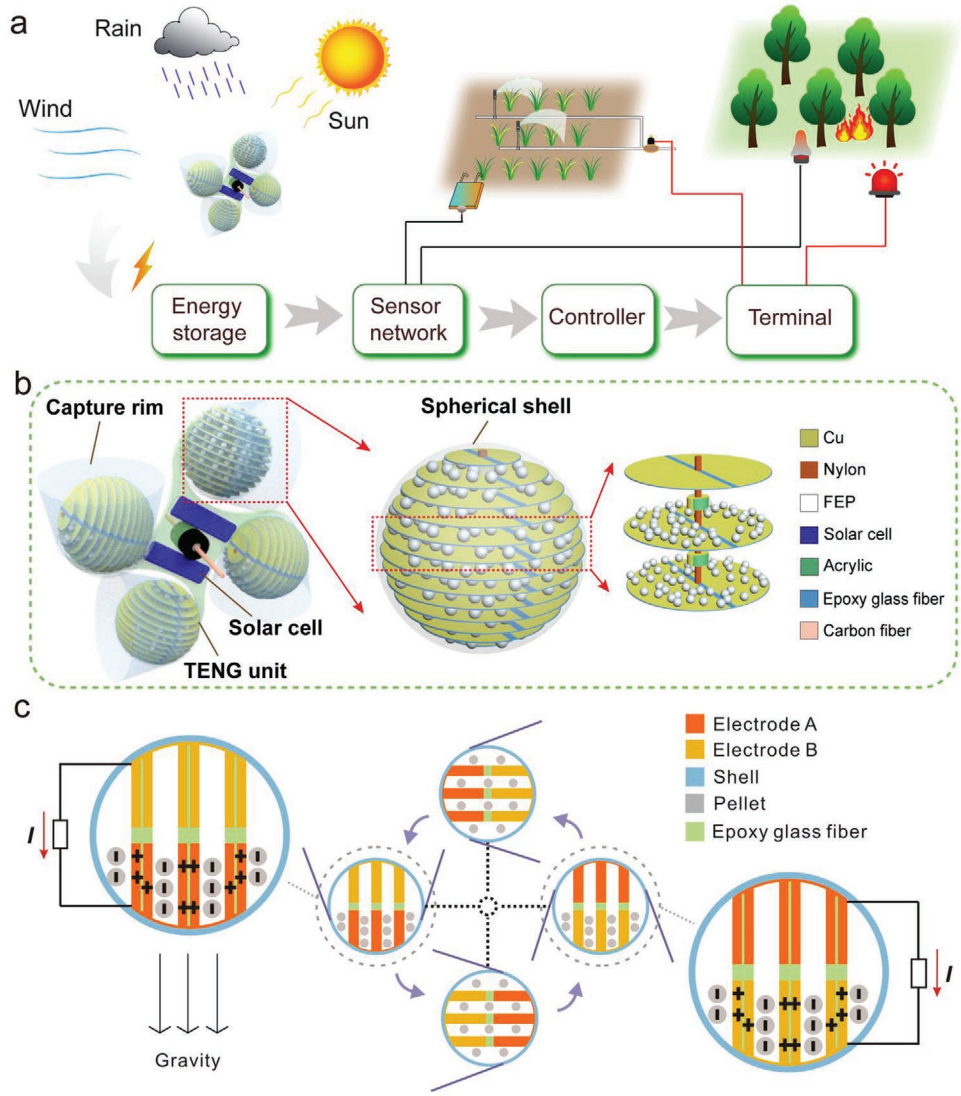

Figure 1. Concept, structure and working principle of the hybrid all-in-one power source (AoPS) for harvesting environmental energy. a) General framework of the AoPS and the environmental self-powered system. b) Structure of the AoPS. c) Working principle of a single TENG unit.

a behavior of going back and forth between the two total electrodes. Owning to the higher affinity to negative charges, the surface of FEP pellets will be negatively electrified.[37] The relative motion of the charged FEP pellets will induce free electrons to move accordingly between the two total electrodes, producing an alternating current in the external circuit. Therefore, the mechanical energy is converted to electricity.

2.3. Fundamental Output Characteristics of the TENG Unit

The energy harvesting of the TENG unit mainly relies on the rotation of the symmetrical structure. To obtain the fundamental characteristics, the output under different rotation speed controlled by a motor was investigated first. **Figure 2**a shows the photograph of the as-fabricated AoPS. Considering the symmetry of the structure, the output measurement of a single TENG unit is representative. The short-circuit current (I_{SC}), short-circuit transferred charges (Q_{SC}) and open-circuit voltage (V_{OC}) of a TENG unit were characterized as shown in Figure 2b–d. With the rotation speed rising from 40 to 140 rpm, the I_{SC} first increase to 3.76 µA at 100 rpm, and then decrease. The Q_{SC} and V_{OC} show a stable output at first, which descends gradually for higher speed. The maximum Q_{SC} and peak-to-peak V_{OC} are 0.47 µC and 5240 V, respectively. The decrease observed here can be attributed to the suppressed motion of the pellets, which results from higher friction by larger centrifugal force, as demonstrated in Figure S1 with supplementary discussion in the Supporting Information. Considering the device usually cannot reach such a high rotation speed in the environment, the decrease will have little influence to practical performance. Meanwhile, lubrication approaches can be adopted to lower the friction, which can also enhance the output at high speed.[38] The output of one TENG unit with various external resistive loads was also investigated. For a rotation speed of 100 rpm, the dependence of the peak current (I_{peak}), peak power

© 2020 Wiley-VCH GmbH

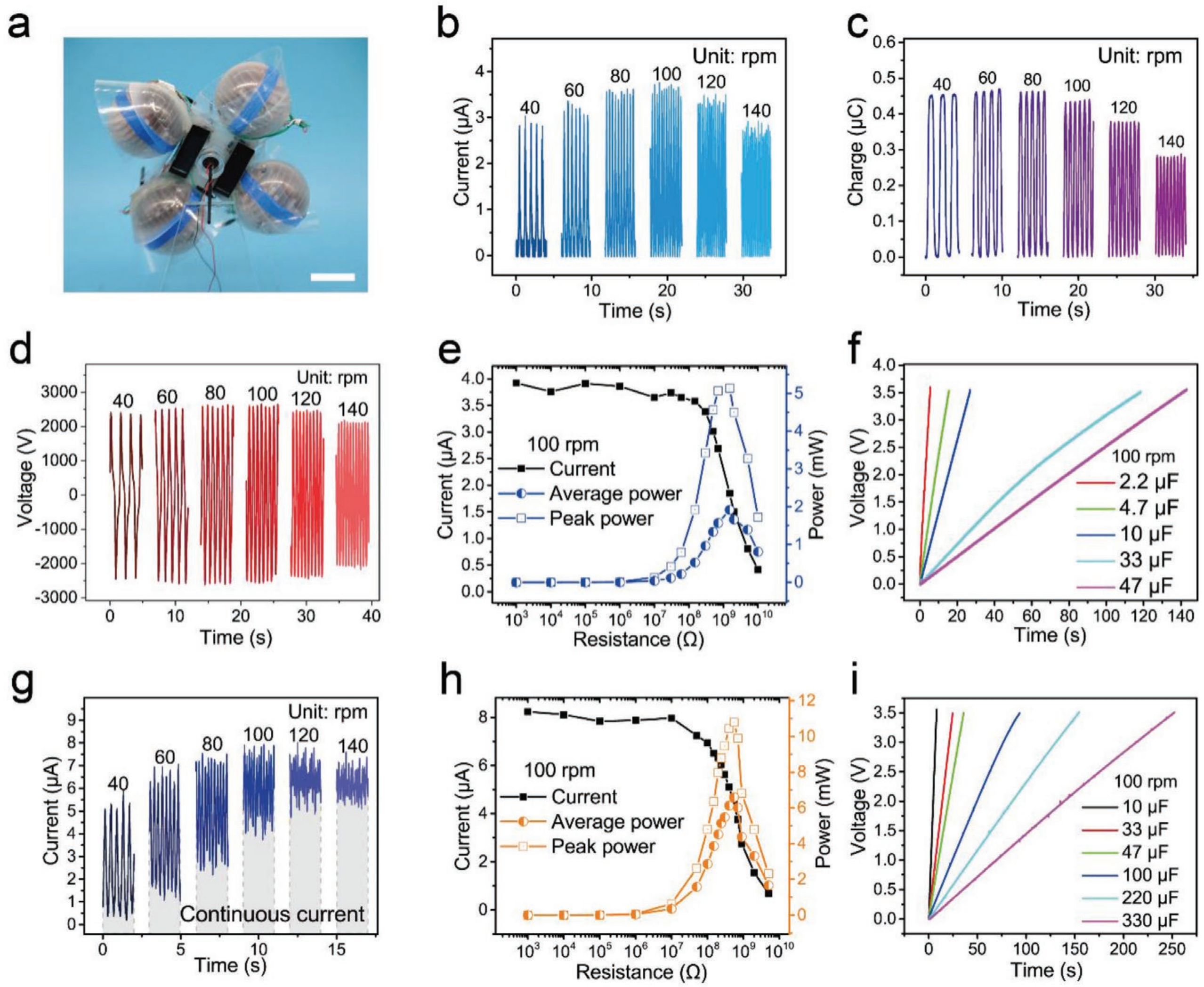

Figure 2. Electrical characterization of the TENG unit. a) Photograph of the as-fabricated AoPS. Scale bar: 5 cm. b) Rectified short-circuit current, c) transferred charges, and d) open-circuit voltage of a single TENG unit with different rotation speeds. e) Current and power output of a single TENG unit under different loads. f) Charging curves of different capacitors with a single TENG unit. g) Short-circuit current of four parallel-connected TENG units under different rotation speeds. h) Current and power output of four TENG units under different loads. i) Charging curves of different capacitors with four TENG units.

(P_{peak}) and average power (P_{ave}) on different resistive loads R is shown in Figure 2e. The P_{ave} is calculated according to the following equation

$$P_{ave} = \frac{\int_0^T I^2 R \mathrm{d}t}{T} \tag{1}$$

where I is the output current, and T is the period of the output. A maximum P_{peak} of 5.13 mW and maximum P_{ave} of 1.93 mW were attained with a resistance of 1.5 GΩ. Figure 2f presents the charging performance of the TENG unit for different capacitors. Under the rotation speed of 100 rpm, a 47 µF capacitor can be rapidly charged to 3.55 V within 143 s.

The output performance can be enhanced by parallel connection of TENG units. For the AoPS, four TENG units are rectified and connected in parallel to deliver a much larger output. Figure 2g shows the rectified I_{SC} for the four TENG units in the AoPS. The current is no longer a typical pulsed signal, but with evident continuous direct current features, and little fluctuations can be observed for high-speed cases. The I_{SC} reaches a maximum of about 7.92 µA under 100 rpm. The power output and charging performance are also effectively enhanced, as shown in Figure 2h,i. A maximum P_{peak} of 10.79 mW and maximum P_{ave} of 6.59 mW are attained with a resistive load of 550 MΩ, under the rotation speed of 100 rpm. And a 47 µF capacitor can be rapidly charged to 3.5 V within 36 s, which means a much higher charging rate.

2.4. Driving Force on TENG Units

In real windy or rainy conditions, the AoPS will be driven to rotate around its flexible shaft. The driving force is analyzed

© 2020 Wiley-VCH GmbH

here for better comprehension of its working mechanism in real environment. First, the driving force from wind is investigated. As schematically shown in Figure S2 (Supporting Information), with wind from a certain direction, the capture rim opening to the wind will block the air and obtain a reacting force that can impose a torque on the whole structure via the arm, and capture rims of other orientations will gain little force. The resulted net torque will make the structure to rotate. To verify this mechanism, the force exerted on the TENG unit with the capture rim was tested. Considering the symmetric characteristic, three representative orientations (noted as 0°, 90°, and 180°) of the single TENG unit were characterized, as shown in **Figure 3**a. During the experiment, the TENG unit was stuck on a forcemeter placed horizontally in the wind. Different wind speeds were generated by an air blower and the corresponding force was recorded. As shown in Figure 3b, with rising wind speed, the measured force also increases. The force for the situation of 0°, which represents an orientation with the capture rim opening to the wind, is much larger than other two situations (90° and 180°) under different wind speeds. With a wind speed around 7.5 m s^{-1}, the force in 0° situation (0.346 N) is about six times of the force in 90° and 180° (0.057 N). Considering a typical state for the AoPS shown in Figure S2 (Supporting Information), the four TENG units are in orientations of 0°, 90°, 180°, and 270°, respectively. The units of 90° and 270° should have very small moment arms and similar forces considering the symmetry. The units of 0° and 180° should have the same moment arm, with a much larger force for 0°. Thus a net torque can be effectively generated. Other states in the rotation of the AoPS can be analyzed similarly. It should be emphasized that no matter what direction the wind is coming from, the AoPS will spin towards the same rotational direction.

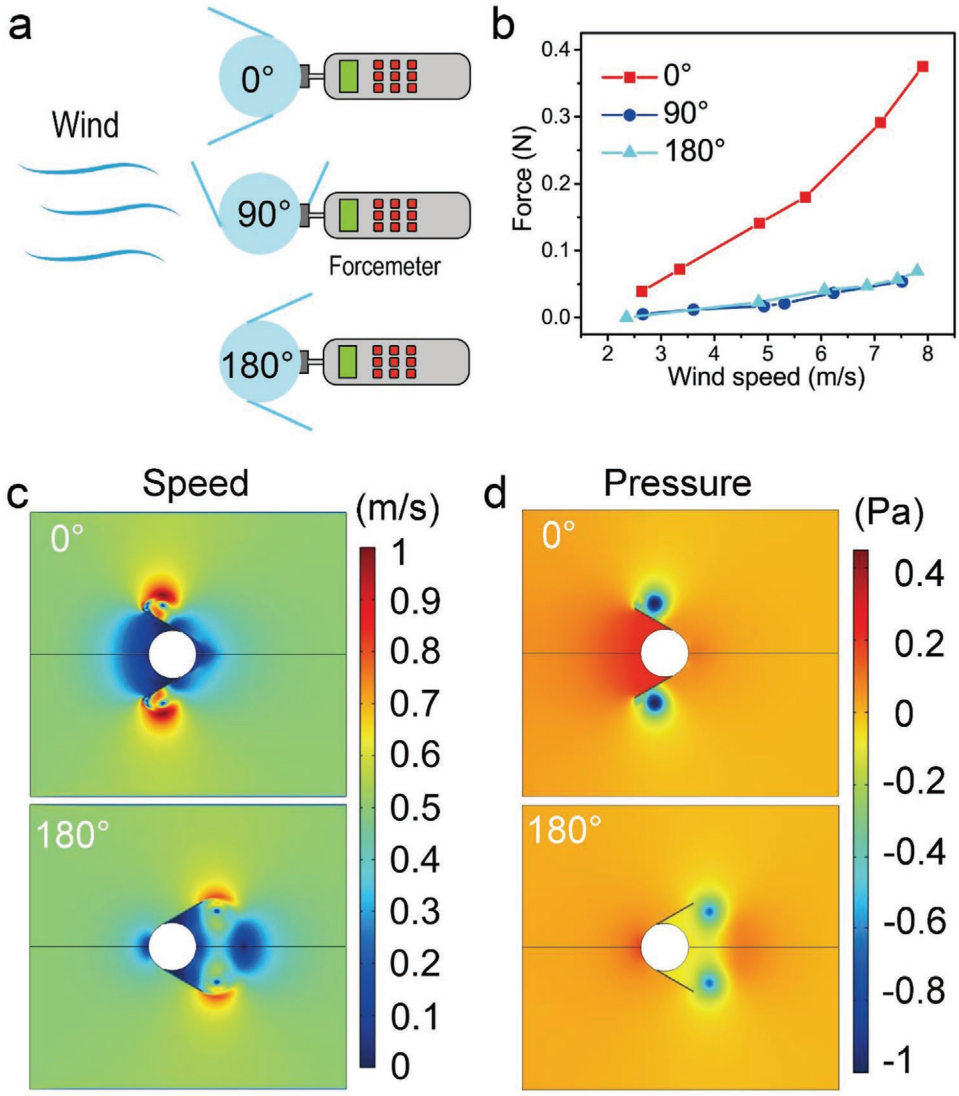

Figure 3. Force analysis of the TENG unit in the wind. a) Schematic diagram of testing the force on the TENG unit with different orientations in the wind. b) The force on the TENG unit with three different orientations in the wind. c) Distribution of horizontal flow speed under the wind of 0.5 m s^{-1} from the left calculated by COMSOL. d) Distribution of relative pressure under the wind of 0.5 m s^{-1} calculated by COMSOL.

 © 2020 Wiley-VCH GmbH

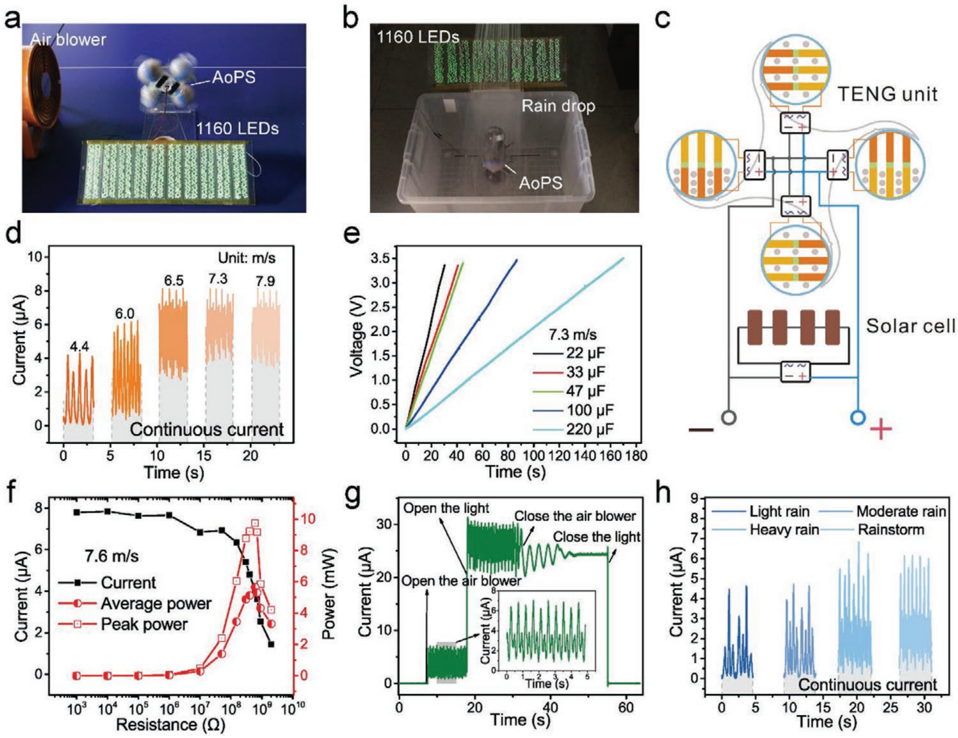

Figure 4. Output performance of the AoPS under various environment conditions. a,b) Photographs of lighting LEDs by the AoPS in the a) wind and b) rain. c) Schematic circuit connection of the AoPS for output. d) Total short-circuit current of the four TENG units with different wind speeds. e) Charging curves of different capacitors with the four TENG units in the wind. f) Current and power output of the four TENG units in the wind under different loads. g) Total short-circuit current of the AoPS in different environment conditions. h) Short-circuit current of the four TENG units in simulated raining conditions.

The fluid flow and air pressure around the TENG unit in the wind were further revealed through FEM calculation based on a commercial software COMSOL. Typical results for a low speed situation (0.5 m s^{-1}) are presented in Figure 3c,d. With the wind from the left side, the distribution of horizontal flow speed for the 0° situation clearly demonstrates a blocking effect of the capture rim on the air flow, and the flow at the outer edge is accelerated (Figure 3c). The distribution of relative pressure shows that the capture rim in the 0° situation will have a much higher pressure at the left side and a much lower pressure at the right side than the 180° situation (Figure 3d), generating a far larger force.

For the rainy condition, as shown in Figure S3 (Supporting Information), the rain drops will be caught and accumulated in the capture rim facing upward. The gravity of the collected water will impose a toque to drive the rotation of the AoPS. Moreover, the impact of the rain drops may also contribute to the rotation.

2.5. Output Performance of the AoPS under Various Environment Conditions

In order to obtain the output performance of the AoPS in real environment, different conditions were simulated in the laboratory for characterization. An air blower and a shower were used for simulating windy and rainy environments respectively. As intuitive demonstrations for its high output, the AoPS (without connecting the solar cells) is shown to be fully capable of lighting up 1160 light-emitting diodes (LEDs) in the wind or rain (**Figure 4**a and Video S1 (Supporting Information) for the wind case, Figure 4b and Video S2 (Supporting Information) for the rain case). The capability of working normally in the rain also indicates the effective packaging of the device for severe environments such as high humidity situations. By further utilizing four commercial solar cells, all typical environmental energies can be simultaneously collected by the AoPS, which allows all-weather energy harvesting. Figure 4c shows the basic circuit diagram for the whole AoPS device hybridizing high-performance spherical TENG units and solar cells. Each TENG unit and series-connected solar cells are wired to the total output via a rectifier respectively.

The output performance of the AoPS in different wind speeds was characterized first without connecting the solar cells. The relationship between the wind speed and the rotation speed of the AoPS is presented in Figure S4 (Supporting Information). As shown in Figure 4d, the output current increases with rising wind speed and obvious continuous direct current feature can be observed. Under a wind speed of 7.3 m s^{-1}, the peak value of the I_{SC} reaches 8.12 μA. Higher wind speed could bring some decay of output due to large rotation speed as discussed above. Under the optimized wind speed of 7.3 m s^{-1}, a 220 μF capacitor can be rapidly charged to 3.51 V within 171 s,

© 2020 Wiley-VCH GmbH

as shown in Figure 4e. The power output of the AoPS driven solely by wind (7.6 m s^{-1}) was also measured. A maximum P_{peak} of 9.74 mW and maximum P_{ave} of 5.63 mW were attained (Figure 4f).

The hybrid performance of the AoPS with solar cells is shown in Figure 4g. In short-circuit state, the AoPS started to output ripple current which peaked at about 7 µA when the air blower was open to produce wind. Then a bias was superposed in the current when light of around 300 lux was applied, achieving a peak value of about 30.3 µA. As observed in the experiment, the rotation of solar cells also can produce some ripples to the current due to small variations of light. By closing the air blower, the current becomes solely from the solar cell, with a decreased value of 24.3 µA, which vanished as the light was turned out. Figure 4h demonstrates the output of the AoPS driven only by simulated rain of four qualitative degrees, which correspond to rotation speeds of about 23, 26, 45, 52 rpm, respectively. The I_{SC} increases with higher intensity of rain, mainly due to larger rate to accumulate rainwater in the capture rim, achieving a peak current of about 6.1 µA with the largest degree. A 47 µF capacitor can be charged to 2.1 V within 274 s under such rain, as shown in Figure S5 (Supporting Information). Successful collecting energy from wind, sun and rain fully demonstrates the feasibility of the AoPS as an all-weather environmental energy harvester that can be adaptive to various conditions.

2.6. Demonstration of the AoPS for Applications

Figure 5a schematically shows the fundamental structure of a practical self-powered monitoring system based on the AoPS. The environmental energy is harvested by the AoPS and stored in the energy storage capacitor, which is used to drive sensors. The signal from the sensor can be further transmitted and analyzed with extensions, such as modules of data acquisition and transmission and computers. In this way, various information from the environment can be collected by a self-powered manner, and processed for feedback actions. Figure 5b shows typical performance of the whole AoPS in charging a capacitor in simulated environment. The solar cell can charge the

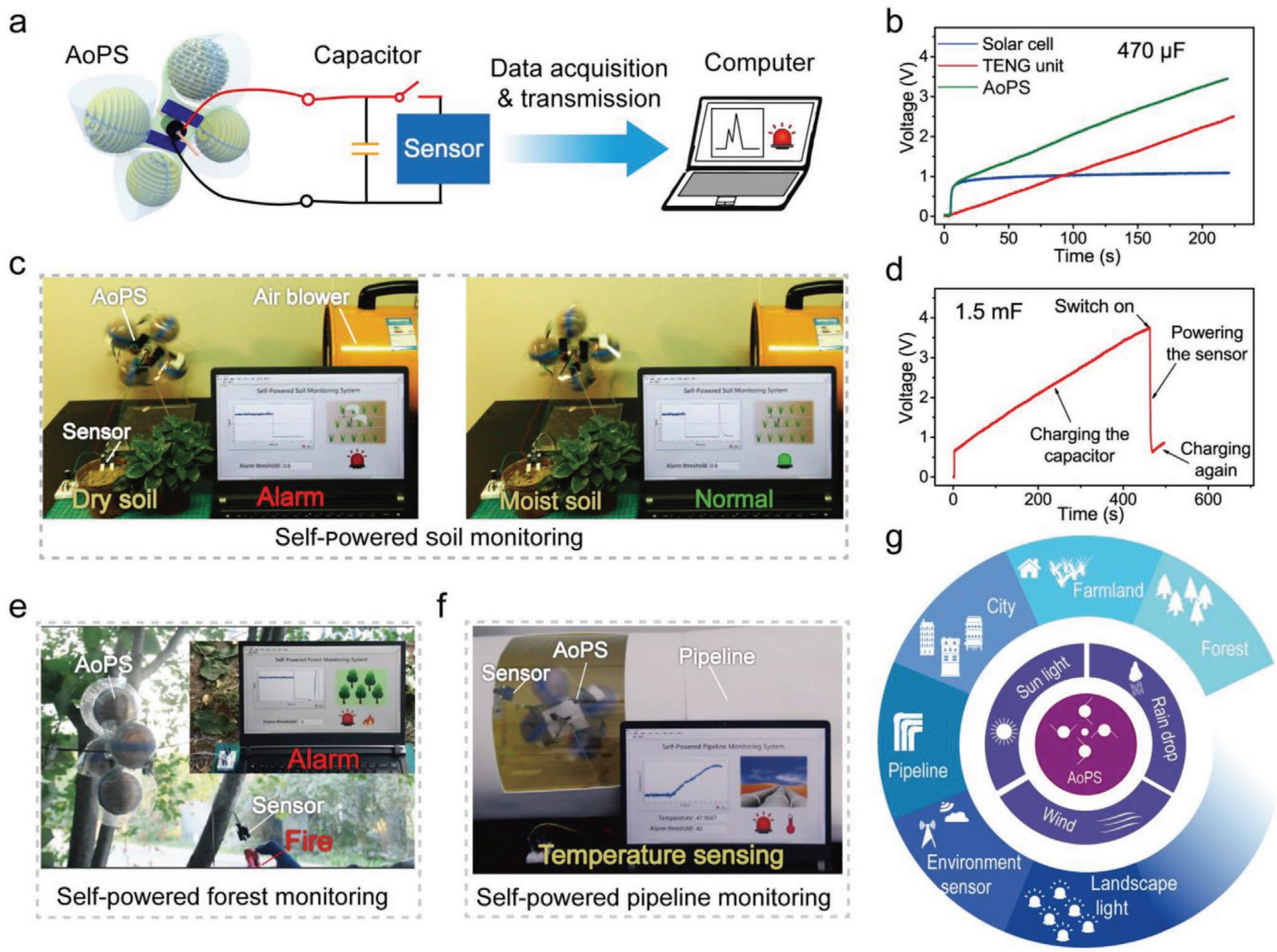

Figure 5. Demonstration of the AoPS for applications. a) Fundamental structure of practical self-powered monitoring systems based on the AoPS. b) Charging curves of the capacitor by the AoPS for powering electronics. c) Photographs of self-powered soil monitoring. d) Voltage variation of the storage capacitor in soil monitoring. e) Photograph of self-powered forest monitoring. f) Photograph of self-powered pipeline monitoring. g) Prospect of the application of AoPS.

© 2020 Wiley-VCH GmbH

capacitor with high charging rate. However, the voltage is limited, while the TENG units can charge the capacitor to much larger voltages. Thus the AoPS can take advantage of both the two types of fundamental devices.

Benefit from the high-performance hybrid design and packaged structure, the system can be quite adaptive to different environments. Here, three typical scenarios are demonstrated. As shown in Figure 5c, a self-powered soil monitoring system for intelligent farm irrigation was constructed. A soil moisture sensor (Youchuang Co., Ltd.) is powered by the AoPS with a 1.5 mF storage capacitor. The information on soil condition will be sensed periodically and transmitted to a program on a computer via a data acquisition card (The program interface is shown in Figure S6, Supporting Information). If the soil is too dry and the moisture is below the threshold, the red alarm for watering will be triggered, which can turn green when the moisture goes above the threshold again through watering. More details are presented in Video S3 (Supporting Information). Figure 5d shows the voltage of a 1.5 mF capacitor in a sensing cycle which can be charged to 3.74 V in 462 s by the AoPS to supply power for accomplishing one sensing action. Considering the soil moisture will not turn to the dry state abruptly, the intermittent working mode is enough for the monitoring. In Figure 5e and Video S4 (Supporting Information), a self-powered forest monitoring system is demonstrated, which can use environmental energy for forest fire detection. A fire alarm will be prompted on the program when abnormality is detected by the fire sensor (Youchuang Co., Ltd.) (The program interface is shown in Figure S7 in Supporting Information). The hybrid design makes the AoPS highly adaptive to different forest conditions, where solely solar cells could be not enough due to rare sun light in some dense forests. Meanwhile, to enhance the output, AoPS arrays can be adopted, and two types of arrays are schematically shown in Figure S8 (Supporting Information). Pipeline is another typical scenario, where there is no light and the environment can be severe with fluid. A self-powered system that adopts flow energy for monitoring fluid temperature in the pipeline is demonstrated in Figure 5f and Video S5 (Supporting Information). The temperature can be collected by the temperature sensor (Youchuang Co., Ltd.) and displayed on the program, which will alarm on abnormal conditions (The program interface is shown in Figure S9, Supporting Information). Figure 5g briefly presents the prospect of the AoPS as a widely adaptive power source in the environment. The three environmental energy sources can be harnessed by the AoPS and eventually serve to the humanity from different aspects, providing a reliable foundation for the era of IoTs.

3. Conclusions

In summary, a hybrid all-in-one power source (AoPS) is demonstrated for widely adaptive environmental energy harvesting. With rationally designed structure, the AoPS hybridize high-performance spherical triboelectric nanogenerators with solar cells, enabling harvesting typical environmental energies from wind, rain drop, and sun light. The spherical structure of the TENG unit with the capture rim allows effectively collecting energy from fluid, such as wind and rain. Nearly continuous direct current and high average power of 5.63 mW can be obtained for four TENG units in the wind, and 1160 LEDs can be lighted up by the TENG units. The force and detailed fluid flow is also analyzed based on experiments and FEM calculation. Moreover, the packaged structure of the TENG units ensures the robustness of the device in severe environment. By complementing with solar cells, the whole AoPS can act as a reliable power source adaptive to different environments with unstable environmental energy condition and effectively supply power for electronics. Typical application scenarios are also demonstrated, achieving self-powered soil moisture control, forest fire prevention and pipeline monitoring. The work proposes and realizes the concept of environmental power source that can be deployed in the environment with high adaptability to make use of all kinds of surrounding energies for sustaining electronics in all-weather condition, showing great application potential for various distributed environmental devices in the era of IoTs.

4. Experimental Section

Fabrication of the TENG Unit: The electrode disks were prepared through printed circuit board (PCB) techniques, with copper electrodes plated on both sides of the epoxy glass fiber sheet. The acrylic spacers (5 mm in thickness and 10 mm in diameter) were cut by a laser cutter (PLS6.75) and two pieces of copper tape were attached on the edge of each spacer for electrical conduction. The nylon rod was used to string them together which was screwed on two sides to form the multilayer structure. FEP pellets with a diameter of 4 mm were filled between the electrode disks and occupied about half the space. Finally, the entire structure was tightly sealed in the spherical PP shell (70 mm in diameter), which was combined by two hemispherical shells. The seam of the PP shell was sealed with water-proof glue, which was wrapped by heat shrinkable tube to avoid peeling-off.

Fabrication of the Capture Rim: The capture rim is made from PET film with a thickness of 0.14 mm. First, the PET film was cut into a shape of sector ring using a laser cutter (PLS6.75), with outer radius 14 cm, width 5.5 cm and central angle $2\pi/3$. Then the film was rolled and pasted into a truncated-cone-shaped structure, which was adhered to the TENG unit.

Integration of the AoPS: First, four TENG units were fixed to the acrylic frame with four arms using hot melt adhesive. Four commercial solar cells (TELESKY) and rectifiers were attached on the two sides of the acrylic frame. Then the circuit was connected correspondingly and output through a slip ring in the center of the acrylic frame (The slip ring can be removed when better packaging is required). The flexible shaft of carbon fiber bore the whole structure through the slip ring solely as a rotation axis. To ensure the water-proof performance, silicone rubber was used to seal electronics.

FEM Calculation: The FEM calculation of the fluid flow and air pressure around the TENG unit in the wind was based on a commercial software COMSOL. In the model, the TENG unit was placed in a wind field with a diameter of 60 cm, and 2D axis symmetry was applied in the calculation. The wind speed at the inlet is 0.5 m s^{-1}.

Characterization: The current, transferred charges and capacitor voltage were measured by an electrometer (Keithley 6514). The open-circuit voltage was measured using an electrostatic voltmeter (Trek 347). Regular rotation was imposed by a motor (PC MOTOR) with adjustable speed. The wind was produced by a commercial air blower, and the rain was simulated by a shower. The force on the TENG unit in the wind was tested by a forcemeter (HP-20N). The wind speed was tested by an anemometer (THINRAD TA-1). The light intensity in the environment was measured with a luxmeter (UNI-T UT383).

© 2020 Wiley-VCH GmbH

Supporting Information

Supporting Information is available from the Wiley Online Library or from the author.

Acknowledgements

The research was supported by National Natural Science Foundation of China (No. 51605033, 51432005), National Key R & D Project from Minister of Science and Technology, China (No. 2016YFA0202704), Youth Innovation Promotion Association, CAS (No. 2019170), China Postdoctoral Science Foundation (No. BX20190324), and Beijing Municipal Science & Technology Commission (No. Z171100002017017).

Conflict of Interest

The authors declare no conflict of interest.

Author Contributions

L.Y.X., L.X., and J.L. contributed equally to this work. L.X. and Z.L.W. conceived the idea. L.X. and L.Y.X. designed the device. L.Y.X. and X.Y. fabricated the device. L.Y.X., J.L., L.X., and B.J. did the experiment. L.Y.X., Y.Y., and L.X. did the FEM calculation. L.Y.X., L.X., J.L., Y.G., and Z.L.W. discussed the data and prepared the manuscript. Z.L.W. and Y.G. guided the whole project.

Keywords

energy harvesting, environmental power sources, triboelectric nanogenerators

Received: May 18, 2020
Revised: July 14, 2020
Published online:

[1] D. Butler, *Nature* **2006**, *440*, 402.
[2] E. Borgia, *Comput. Commun.* **2014**, *54*, 1.
[3] J. Jin, J. Gubbi, S. Marusic, M. Palaniswami, *IEEE Internet Things* **2014**, *1*, 112.
[4] D. Larcher, J. M. Tarascon, *Nat. Chem.* **2015**, *7*, 19.
[5] F. R. Fan, Z. Q. Tian, Z. L. Wang, *Nano Energy* **2012**, *1*, 328.
[6] L. Xu, T. Jiang, P. Lin, J. J. Shao, C. He, W. Zhong, X. Y. Chen, Z. L. Wang, *ACS Nano* **2018**, *12*, 1849.
[7] J. Bae, J. Lee, S. Kim, J. Ha, B. S. Lee, Y. Park, C. Choong, J. B. Kim, Z. L. Wang, H. Y. Kim, J. J. Park, U. I. Chung, *Nat. Commun.* **2014**, *5*, 4929.
[8] Z. H. Lin, G. Cheng, S. Lee, K. C. Pradel, Z. L. Wang, *Adv. Mater.* **2014**, *26*, 4690.
[9] C. S. Wu, A. C. Wang, W. B. Ding, H. Y. Guo, Z. L. Wang, *Adv. Energy Mater.* **2019**, *9*, 1802906.
[10] R. Hinchet, H. J. Yoon, H. Ryu, M. K. Kim, E. K. Choi, D. S. Kim, S. W. Kim, *Science* **2019**, *365*, 491.
[11] L. Xu, T. Z. Bu, X. D. Yang, C. Zhang, Z. L. Wang, *Nano Energy* **2018**, *49*, 625.
[12] Z. L. Wang, *Mater. Today* **2017**, *20*, 74.
[13] S. M. Niu, Z. L. Wang, *Nano Energy* **2015**, *14*, 161.
[14] J. Chen, G. Zhu, W. Q. Yang, Q. S. Jing, P. Bai, Y. Yang, T. C. Hou, Z. L. Wang, *Adv. Mater.* **2013**, *25*, 6094.
[15] X. D. Yang, L. Xu, P. Lin, W. Zhong, Y. Bai, J. J. Luo, J. Chen, Z. L. Wang, *Nano Energy* **2019**, *60*, 404.
[16] B. Chen, Y. Yang, Z. L. Wang, *Adv. Energy Mater.* **2018**, *8*, 1702649.
[17] J. J. Luo, W. Tang, F. R. Fan, C. F. Liu, Y. K. Pang, G. Z. Cao, Z. L. Wang, *ACS Nano* **2016**, *10*, 8078.
[18] J. Q. Xiong, P. Cui, X. L. Chen, J. X. Wang, K. Parida, M. F. Lin, P. S. Lee, *Nat. Commun.* **2018**, *9*, 4280.
[19] S. Chun, C. Pang, S. B. Cho, *Adv. Mater.* **2020**, *32*, 1905539.
[20] Q. J. Liang, X. Q. Yan, X. Q. Liao, Y. Zhang, *Nano Energy* **2016**, *25*, 18.
[21] Y. C. Lai, Y. C. Hsiao, H. M. Wu, Z. L. Wang, *Adv. Sci.* **2019**, *6*, 1801883.
[22] Y. L. Zi, J. Wang, S. H. Wang, S. M. Li, Z. Wen, H. Y. Guo, Z. L. Wang, *Nat. Commun.* **2016**, *7*, 10987.
[23] H. Ryu, J. H. Lee, U. Khan, S. S. Kwak, R. Hinchet, S. W. Kim, *Energy Environ. Sci.* **2018**, *11*, 2057.
[24] J. J. Luo, Z. M. Wang, L. Xu, A. C. Wang, K. Han, T. Jiang, Q. S. Lai, Y. Bai, W. Tang, F. R. Fan, Z. L. Wang, *Nat. Commun.* **2019**, *10*, 5147.
[25] J. J. Luo, Z. L. Wang, *Energy Storage Mater.* **2019**, *23*, 617.
[26] Y. Bai, L. Xu, C. He, L. Zhu, X. Yang, T. Jiang, J. Nie, W. Zhong, Z. L. Wang, *Nano Energy* **2019**, *66*, 104117.
[27] X. Pu, L. X. Li, H. Q. Song, C. H. Du, Z. F. Zhao, C. Y. Jiang, G. Z. Cao, W. G. Hu, Z. L. Wang, *Adv. Mater.* **2015**, *27*, 2472.
[28] Z. Wen, M. H. Yeh, H. Guo, J. Wang, Y. Zi, W. Xu, J. Deng, L. Zhu, X. Wang, C. Hu, *Sci. Adv.* **2016**, *2*, e1600097.
[29] X. Pu, W. Song, M. Liu, C. Sun, C. Du, C. Jiang, X. Huang, D. Zou, W. Hu, Z. L. Wang, *Adv. Energy Mater.* **2016**, *6*, 1601048.
[30] U. T. Jurado, S. H. Pu, N. M. White, *Nano Energy* **2020**, *72*, 104701.
[31] Y. Yang, H. Zhang, J. Chen, S. Lee, T. C. Hou, Z. L. Wang, *Energy Environ. Sci.* **2013**, *6*, 1744.
[32] D. Jiang, Y. Su, K. Wang, Y. Wang, G. Chen, *Nano Energy* **2020**, *70*, 104459.
[33] Q. Schiermeier, J. Tollefson, T. Scully, A. Witze, O. Morton, *Nature* **2008**, *454*, 816.
[34] Z. L. Wang, *Faraday Discuss.* **2014**, *176*, 447.
[35] V. Nguyen, R. S. Yang, *Nano Energy* **2013**, *2*, 604.
[36] S. Baik, H. J. Lee, D. W. Kim, H. Min, C. Pang, *ACS Appl. Mater. Interfaces* **2019**, *11*, 25674.
[37] H. Y. Zou, Y. Zhang, L. T. Guo, P. H. Wang, X. He, G. Z. Dai, H. W. Zheng, C. Y. Chen, A. C. Wang, C. Xu, Z. L. Wang, *Nat. Commun.* **2019**, *10*, 1427.
[38] J. Wu, Y. Xi, Y. Shi, *Nano Energy* **2020**, *72*, 104659.

© 2020 Wiley-VCH GmbH